

# Semi-Analytical Calculation of the Rouse Dynamics of Randomly Branched Polymers

Josh P. Kemp, Zheng Yu Chen

*Guelph-Waterloo Program for Graduate Work in Physics and Department of Physics, University of Waterloo, Waterloo, Ontario, Canada N2L 3G1*

(February 1, 2008)

We present a semi-analytical approach to the determination of the dynamic properties of randomly branched polymers under the Rouse approximation. The principle procedure is based on examining a spectrum of eigenvalues which represents the average dynamic behavior of various structures. The calculated spectra show that the eigenvalue distribution is random even within a single structure which in turn produces a continuous spectrum of values for the entire class. The auto-correlation functions for the radius of gyration squared were calculated based on these spectra, which confirms that the dynamics is non-exponential as earlier reported. A universal stretched exponent is also found in this study.

61.25.Hq, 61.20.Lc, 61.43.Bn

Among macromolecular structures found in many important systems such as plastics, proteins, and sol-gel networks [1–3], randomly branched structures occupy a unique place, as they display distinct physical properties from those of linear or regularly branched polymers. A typical molecule is constructed from a connection of linear polymer portions of various lengths at branching sites selected randomly according to the underlying physical branching mechanism [see Fig. 1]. The study of randomly branched polymers (RBPs) poses an interesting challenge to condensed matter theorists, as the average over many different branching structures must be included in addition to the ensemble average taken over the configurational space for a given single structure. Most of the previous studies on these polymers have been focused on their conformational properties [4–6], which reveal different scaling properties from linear polymer chains. The more intriguing aspect of randomly branched polymers is probably their connection to the spin glass problem: there exists a difference in quenched and annealed disorders, typical to random systems [5,6]. The dynamic properties of these polymers, however, remains largely unexplored.

In a recent study [7], we were able to show, with the aid of Monte Carlo computer simulations, that the dynamic behavior of these polymers in a good solvent does not exhibit the conventional exponential relaxation normally seen in other regularly branched structures. The difficulty associated with the dynamic study of this class of polymer is that each polymer has a unique dynamic behavior dependent on its structure. Although the structural averages can be performed using various techniques developed in statistical physics [6], it is unclear how to construct a rigorous analytical theory to explain the dynamic properties even for the simplest cases, which have been examined by using scaling arguments [1,7]. In principle, numerical simulations of polymers provide an alternative approach for examining the basic dynamic behavior of these randomly branched structures, allowing the sampling of many different branching structures. In

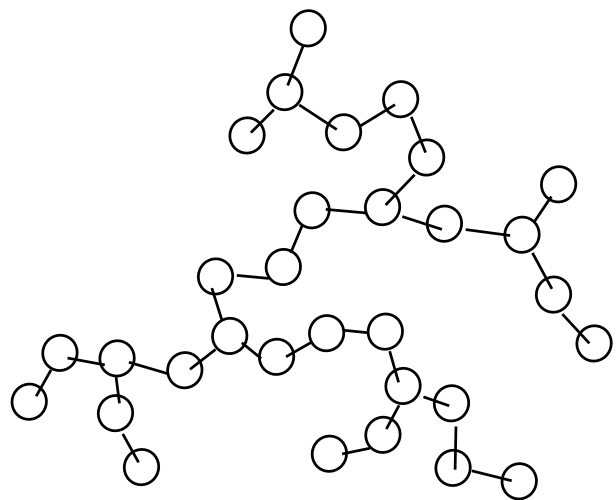


FIG. 1. Sketch of a typical randomly branched polymer.

practice, however, the number of branching structures that can be sampled is limited, due to the extensive computational time required.

There are many unaddressed questions regarding the dynamics of RBPs. For example, one simple question is whether or not the non-exponential behavior is indeed an intrinsic property of the randomness. If it is, then it will show up inherently even in the simplest type of polymer dynamics, the Rouse dynamics, where the excluded volume and hydrodynamic interactions are both neglected. In this article, we examine the Rouse dynamics of an autocorrelation function and intrinsic viscosity of RBPs using a semi-analytical method with a satisfactory average over the structural space.

For a given structure, the Rouse dynamics are characterized by a  $N \times N$  Rouse force matrix  $A$  appearing in the Langevin equation [10],

$$\zeta \frac{d\vec{r}}{dt} = kA\vec{r} + \vec{f}(t) \quad (1)$$

where  $\zeta$  is the inverse mobility,  $\vec{r}$  is a  $N$ -dimensional vector containing the positional coordinates of the  $N$

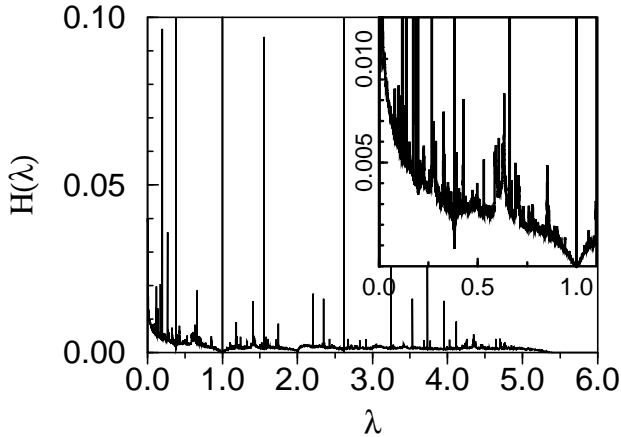


FIG. 2. The average eigenvalue spectrum for RBPs of  $N = 100$ . The spectrum appears continuous suggesting that the eigenvalues are distributed randomly for a single structure. The inset graph shows dominating eigenvalues in the long time scale, and emphasizes the continuous distribution of the modes. The five peaks which extend beyond the range of the main graph, reach values of approximately 0.7, 2.5, 0.7, 0.1, and 0.03, from left to right.

monomers, and  $\vec{f}(t)$  is a  $N$ -dimensional random force vector containing Brownian forces acting on these  $N$  monomers. The  $N$  eigenvalues of  $A$  determine the relaxation rate and dynamic properties of various collective normal modes of the given structure.

The matrix  $A$  is directly determined by how the structure (Fig. 1) is labeled and connected, which is analytically generated here by a cut and paste algorithm, similar to the one used by Cui and Chen [5]. Starting from a linear polymer, we choose a bond randomly and cut the molecule into two portions. The smaller portion was then attached to a randomly chosen monomer on the larger portion. The move was discarded if the anticipated bonding site was already a branching monomer. The spatial positions of the monomers were not kept track of as the Rouse matrix is only concerned with the connectivity of the structure when the monomers have no volume. The process was initially repeated  $10^5$  times to create an equilibrate structure before data collection. This algorithm was originally suggested by Rensberg and Madras [8], in their study of lattice “animals”, and has been shown to yield a branching ratio between the number of branching nodes,  $n_3$ , and total number of bonds,  $N$ , of  $n_3/N \approx 0.25$  [5].

A Rouse matrix was created after every ten cut-paste moves, to ensure that the structures were not all correlated. Once the Rouse matrix was defined, a complete set of eigenvalues were then determined numerically [9], and binned to create a normalized histogram. Each bin was given a width of  $1.0 \times 10^{-4}$  to create a fine scale image of the distribution. For each given  $N$ , a total of  $10^7$  structures were examined.

The spectrum that is produced is distinctly different from that of a linear polymer. The spectrum for a linear

polymer would be constructed of only  $N$  eigenvalues, and thus would appear as  $N$  discrete lines spaced according to the following equation [10],

$$\lambda_p = \lambda_1 p^2 ; p = 1, 2, \dots, N , \quad (2)$$

where  $\lambda_1$  is the smallest eigenvalue. In Fig. 2 the eigenvalue histogram for a RBP structure of  $N = 100$  bonds is displayed. The magnified portion for eigenvalues between 0 and 1, which governs the longest time scales of relaxation, shows that the distribution is continuous, and roughly follows a power law near  $\lambda = 0$ . This histogram distribution indicates that the eigenvalues are uniformly distributed due to various segmental lengths and the coupling of the segments in the molecules. The figure also demonstrates that the eigenvalues of a single structure are randomly distributed, opposed to an ordered distribution as in a linear polymer. These features can be seen more clearly in Fig. 3, where the histogram for  $N=10$  is displayed. In a structure this small there are a limited number of distinct structures, and thus a limited number of possible eigenvalues, so the eigenvalues appear discrete in the spectrum. The figure clearly shows how the eigenvalues are randomly arranged in the spectrum.

Returning to Fig. 2, there appear to be several eigenvalues which occur more frequently than the average. These eigenvalues are most likely caused by frequently occurring sub-structures that are regularly branched or linear. For example, the relative motion of a sub-unit that has two outer monomers connected to a stationary branching unit, will have an eigenvalue of 1 [11]; the large peak indicates the frequent appearance of such units.

One of the most direct probes of the internal structure is the autocorrelation function associated with the radius of gyration squared. As has been appreciated in other

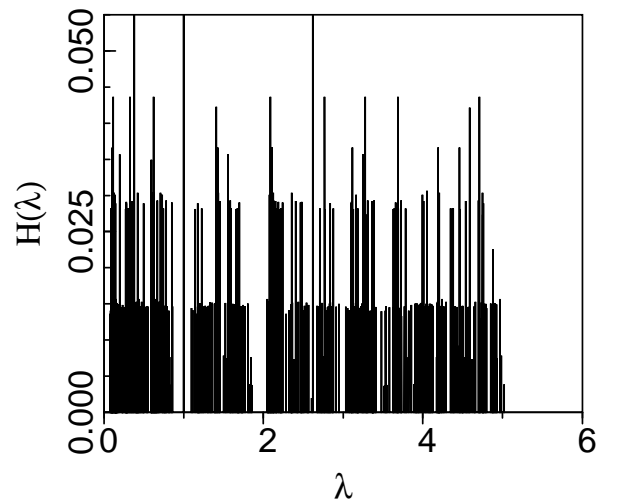


FIG. 3. The average eigenvalue spectrum for RBPs of  $N = 10$ . The small size of the polymer generates a distinctly different spectrum from that in Fig. 2. The spectrum is discrete, yet randomly distributed. This spectrum still generates a non-exponential behavior.

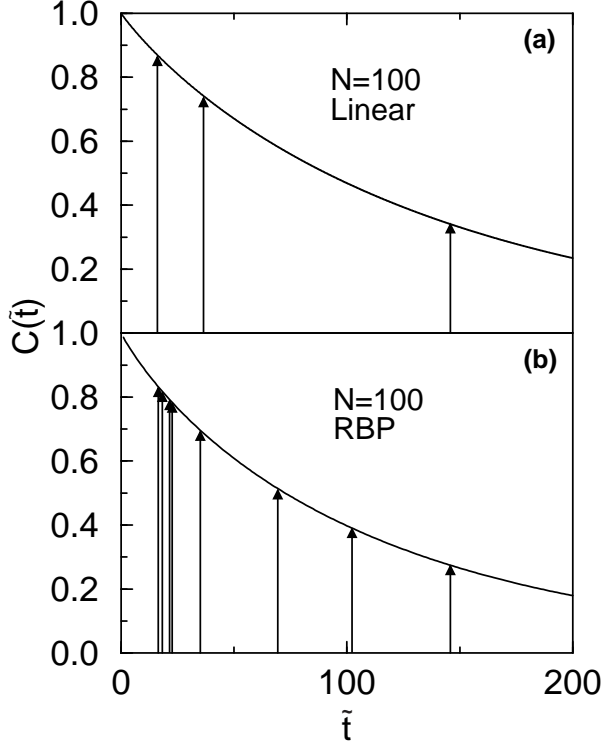


FIG. 4. Auto-correlation functions for a linear polymer (a) and a RBP (b) of length  $N=100$ . The function in (a) has been scaled such that the largest characteristic time,  $\tilde{\tau}_1$ , is set to match that in figure (b). The other largest characteristic times are also placed on the graph to demonstrate their magnitudes. In figure (b), long time relaxation is dominated by multiple modes, which cause the observed non-exponential behavior.

macromolecular structures, such a correlation function characterizes the radial relaxation motion, and defines the so-called elastic relaxation for a macromolecule [12]. The dynamic relaxation of such a correlation is comprised of the various internal relaxation times. Due to the large number of small eigenvalues in a RBP, no eigenvalue can be singled out to yield dominating exponential behavior. More specifically, we examine

$$C(t) = \frac{\langle S^2(t) \cdot S^2(0) \rangle - \langle S^2(0) \rangle^2}{\langle S^2(0) \cdot S^2(0) \rangle - \langle S^2(0) \rangle^2} = \frac{\sum_{i=1}^N \frac{H(\lambda_i)}{\lambda_i^2} e^{-\lambda_i \tilde{t}}}{\sum_{i=1}^N \frac{H(\lambda_i)}{\lambda_i^2}} \quad (3)$$

where  $\tilde{t}$  is the rescaled time such that  $\tilde{t} = 2kt/\zeta$ , and  $H(\lambda_i)$ , represents the probability of the occurrence of the eigenvalue  $\lambda_i$  given by the histogram.

To further illustrate the significance of many time scales involved in the dynamics, the autocorrelation function for the radius of gyration squared (Eq.3) was calculated for a linear polymer and a typical RBP of  $N=100$  monomers in Fig. 4a and Fig. 4b respectively. Also plotted in the figures are the longest characteristic time

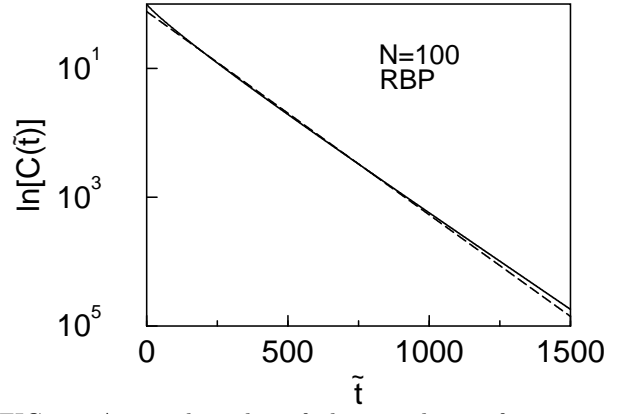


FIG. 5. A semi-log plot of the correlation function vs. rescaled time, for the RBP in figure 4b. The curve is fitted with an exponential function to demonstrate the systematic deviation of the curve from this function, implying a non-exponential relaxational behavior.

scales, indicated by the vertical arrows. The RBP has a significantly shorter relaxation time than the linear polymer since the structure is more compact, thus in the comparison of the distribution of the characteristic times, the linear polymer's time scales have been scaled such that the longest characteristic times of both polymers match exactly. Of course, when  $t$  is extremely large only the largest time scale is dominant, but this only occurs when the correlation is no longer significant, thus the correlation function is dominated by non-exponential relaxation. Comparing the two figures, we see that the characteristic time scales in a linear polymer, in which  $\tau_p = \tau_1 p^{-2}$ ,  $p = 1, 2, \dots, N$  [10], are sparsely spaced in the region of interest, while the time scales in the RBP are irregularly distributed in the same regime. The two or three longest time scales in Fig. 4b, are sufficiently close together to compete with each other; the net result is a multi-exponential function rather than a single exponential function as in Fig. 4a. When averaged over different structures, various long time scales must be taken

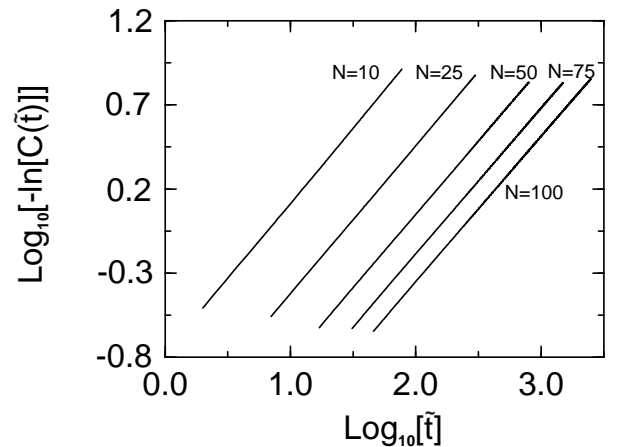


FIG. 6. A double logarithmic plot of the correlation functions, for  $N=10, 25, 50, 75$ , and  $100$ . These plots are used to calculate the parameters  $\alpha$  and  $\tilde{\tau}$  in Eq. (4).

into account, which yields an average over various multi-exponential functions. As discussed by Palmer et al. [13], and Iori et al. [14], such a process produces much slower decaying correlation functions, which sometimes are represented by various non-exponential functions.

The co-operative behavior of the competing time scales can be seen in Fig. 5, from another perspective. The figure shows a semi-log plot of autocorrelation function for the same function in Fig. 4b. The dashed line is the best fit to the solid curve with an exponential function, which demonstrates that the correlation function is not exponential as in linear polymers. This result is in agreement with previous Monte Carlo simulation results which show the same non-exponential relaxation [7].

We have shown thus far that the eigenvalues of RBPs are randomly distributed, and the continuous distribution near  $\lambda = 0$  yields insight into the non-exponential relaxation. Without further knowledge of an analytical expression of  $H(\lambda)$ , the summation in Eq.(3) cannot be carried out exactly. As in previous work [7], due to similarities of this system with spin glass systems and other random disordered systems [13–16], it is instructive to compare the correlation curve to a stretched exponential.

$$C_{st}(\tilde{t}) = e^{[-\tilde{t}/\tilde{\tau}]^\alpha} \quad (4)$$

where  $\tilde{\tau}$  represents a general characteristic time for the entire class of RBPs, and  $\alpha$  is the stretched exponent. As can be inferred from Fig. 6, the stretched exponential function gives a rather good approximation with the curves produced from Eq. (3). The  $\alpha$  values for different  $N$  are shown in Table I, which demonstrates that  $\alpha \approx 0.87 \pm 0.01$  appears universal for all large  $N$  considered here. The range used to calculate the exponents was selected by choosing the range of time scales such that the auto-correlation function was approximately 0.8 to less than  $10^{-4}$ , corresponding to the region where an exponent of one can be produced for linear polymers. This value can be compared with  $\alpha \approx 0.8$  exponent calculated in earlier work [7]; the discrepancy is not surprising since this model considers no excluded volume effects.

To further determine the universality of the stretching exponent  $\alpha$ , we have calculated the eigenvalue spectra for RBPs with a different branching probability, corresponding to  $n_3/N = 1/2$ . In these polymers there exist only end and branching points in the structure, and no linear

TABLE I. Stretched exponents, relaxation times and intrinsic viscosity determined for various  $N$ . These systems correspond to a branching ratio of  $n_3/N \approx 0.25$ .

$N$	$\alpha$	$\tilde{\tau}$	$[\tilde{\eta}]$
10	$0.902 \pm 0.005$	$7.55 \pm 0.05$	$1.49 \pm 0.05$
25	$0.879 \pm 0.005$	$30.2 \pm 0.05$	$2.81 \pm 0.05$
50	$0.871 \pm 0.005$	$87.8 \pm 0.05$	$4.38 \pm 0.05$
75	$0.865 \pm 0.005$	$163.6 \pm 0.05$	$5.63 \pm 0.05$
100	$0.861 \pm 0.005$	$254.2 \pm 0.05$	$6.69 \pm 0.05$

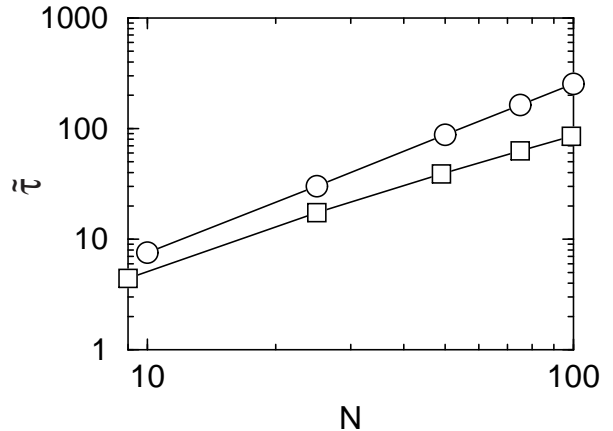


FIG. 7. A log-log plot of  $\tilde{\tau}$  vs.  $N$ . Circles and squares correspond to two different classes of RBPs, those with  $n_3/N = 0.25$  and  $n_3/N = 0.5$  respectively.

parts are allowed. To create these structures, a base star nucleus of 4 monomers was used. Using this base an end monomer was randomly selected and two monomers were attached to change the end monomer to a branching point. This process was repeated until the desired structure size,  $N = 9, 25, 49, 75$ , and  $99$ , was reached. The resulting correlation curves demonstrate the same stretched exponent as in the case of much lower branching probability. The results are shown in Table II. This suggests that there is little or no dependence of the stretching exponent on the branching probability. Also, the examination of the exponents suggests that there is an insignificant correlation with  $N$ , suggesting that this stretching behavior is universal to the entire class of RBPs. Whether the quenched and annealed universality classes [5,6] will produce the same exponents cannot be determined without the introduction of the excluded volume.

The exponent  $\tilde{\tau}$ , displayed in Tables I and II, in equation 4 can also be calculated from Fig. 6. The plot against  $N$  in Fig.7 yields the scaling laws,

$$\tilde{\tau} \sim N^{(1.5 \pm 0.1)} \text{ for } n_3/N \approx 0.25 \quad (5)$$

$$\tilde{\tau} \sim N^{(1.2 \pm 0.1)} \text{ for } n_3/N \approx 0.5 \quad (6)$$

Our early work [7] suggests a larger exponent with the inclusion of an excluded volume interaction. This is consistent with the fact that the excluded volume effect slows down the dynamics generally [17].

TABLE II. Stretched exponents, relaxation times, and intrinsic viscosity for various  $N$ . These systems correspond to a branching ratio of  $n_3/N \approx 0.5$ .

$N$	$\alpha$	$\tilde{\tau}$	$[\tilde{\eta}]$
9	$0.924 \pm 0.005$	$4.4 \pm 0.05$	$1.20 \pm 0.05$
25	$0.874 \pm 0.005$	$17.3 \pm 0.05$	$2.24 \pm 0.05$
49	$0.859 \pm 0.005$	$39.0 \pm 0.05$	$3.15 \pm 0.05$
75	$0.851 \pm 0.005$	$63.0 \pm 0.05$	$3.80 \pm 0.05$
99	$0.846 \pm 0.005$	$85.1 \pm 0.05$	$4.25 \pm 0.05$

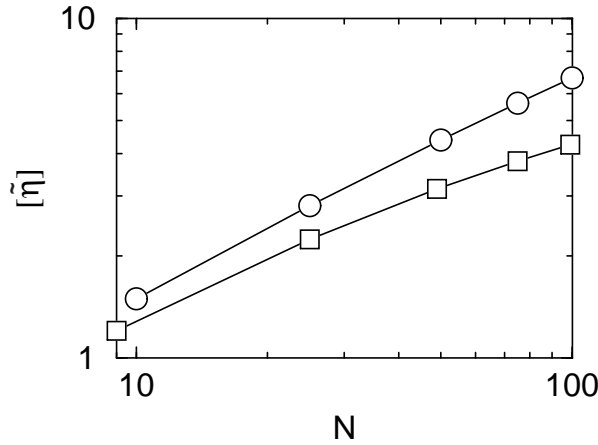


FIG. 8. A log-log plot of the intrinsic viscosity vs.  $N$ . Circles and squares correspond to two different classes of RBPs, those with  $n_3/N = 0.25$  and  $n_3/N = 0.5$  respectively. The straight line represents Eq.(7).

The intrinsic viscosity,  $[\eta]$ , is also a significant probe of the internal dynamics of a macromolecule, and can be directly measured experimentally. One can show that  $[\eta]$  is related to the eigenvalues [18] by

$$[\tilde{\eta}] = \frac{[\eta]6\rho\eta_s}{N_A a^2 \zeta} = \frac{1}{(N+1)} \sum_{i=1}^N \frac{H(\lambda_i)}{\lambda_i} \quad (7)$$

where  $N_A$  is Avogadro's number,  $\eta_s$  is the viscosity of the solvent,  $\rho$  is the weight per monomer, and  $a$  is the intermolecular bonding distance. The rescaled intrinsic viscosities are displayed in Tables I and II. The log-log plot of  $[\tilde{\eta}]$  vs.  $N$  shows

$$[\tilde{\eta}] \sim N^{0.63 \pm 0.01} \text{ for } n_3/N \approx 0.25 \quad (8)$$

$$[\tilde{\eta}] \sim N^{0.47 \pm 0.01} \text{ for } n_3/N \approx 0.5 \quad (9)$$

The exponent calculated here is for a Rouse model dynamics. It is known that under the Rouse approximation, no simple scaling relation between  $[\eta]$  and  $N$  can be deduced. While linear polymers show  $\eta \propto N$ , star-burst dendrimers show  $\eta \propto \ln N$  [11].

In practical good solvents, both hydrodynamic and excluded-volume effects must be considered. In such cases, a simple relationship can be deduced based on the fact that  $[\eta]$  is inversely proportional to the particle density  $S^3/N$ , where  $S$  is the radius of gyration. Based on this scaling argument, Daoud et al. [1] have concluded a scaling exponent of  $3/8$  for  $[\eta]$ , which, of course, cannot be directly compared with the exponent found here due to different physical origins involved. The exponent  $3/8$  agrees with the experimental results of branched polyethylene by Patton et al. [3]. A more rigorous treatment of  $[\eta]$  for RBPs beyond the scaling argument, however, cannot be found in previous literatures.

In summary, by examining the average eigenvalue spectrum of RBPs, we were able to show that the eigenvalues are randomly distributed as opposed to periodically organized. The result of this distribution is the competition of

relaxational modes which leads to a non-exponential behavior in the relaxation of the polymer. Fitting the autocorrelation functions of the radius of gyration squared to a stretched exponential we found a stretching exponent of  $\alpha = 0.87 \pm 0.04$ .

We would like to thank C. Cai for providing the algorithm to calculate the eigenvalues, and S. Dwyer for the critical reading of the manuscript. We would also like to thank the Natural Sciences and Engineering Research Council of Canada for financial support.

- 
- [1] M. Daoud, A. Lapp, J. Phys.: Condens. Matter, **2**, 4021 (1990); M. Daoud, F. Family, G. Jannink, J. Physique Lett., **45** 199 (1984)
  - [2] See eg. P.G. de Gennes, Biopolymers, **6**, 715 (1968); P.L. Privaloo, V.V. Filimonov, J. Mol. Biol., **122**, 447 (1978); P.G. Higgs, J. Phys. (France), **I 3**, 43 (1993)
  - [3] E. Patton, J.A. Wesson, M. Rubinstein, J.C. Wilson, L.E. Oppenheimer, Macromolecules, **22**, 1946 (1989)
  - [4] G. Parisi, N. Sourlas, Phys. Rev. Lett., **46**, 871 (1981); J. Isaacson, T.C. Lubensky, J. Physique Lett., **41**, 469 (1980); T.C. Lubensky, J. Isaacson, Phys. Rev. A, **20**, 2130 (1979); A. Grosberg, A. Gutin, E. Shakhnovich, Macromolecules, **28**, 3718 (1995); A.M. Gutin, A.Y. Grosberg, E.I. Shakhnovich, J. Phys. A **26**, 1037 (1993)
  - [5] S.-M. Cui, Z.Y. Chen, Phys. Rev. E, **53**, 6238 (1996)
  - [6] A.M. Gutin, A.Y. Grosberg, E.I. Shakhnovich, Macromolecules, **26**, 1293 (1993); S.-M. Cui, Z.Y. Chen, Phys. Rev. E, **52**, 5084, (1995)
  - [7] J.P. Kemp, Z.Y. Chen, Phys. Rev. E, **56**, 7017 (1997)
  - [8] E.J. van Rensburg, N. Madras, J. Phys. A, **25**, 303 (1992)
  - [9] W.H. Press, B.P. Flannery, S.A. Teukolsky, W.T. Vetterling, *Numerical Recipes (FORTRAN Version)*, Page 364-367, Cambridge University Press, Cambridge, (1992)
  - [10] M. Doi, S.F. Edwards, *The Theory of Polymer Dynamics*, Clarendon Press, Oxford, 1988
  - [11] C. Cai, Z.Y. Chen, Macromolecules, **30**, 5104 (1997)
  - [12] G.S. Grest, M. Murat, in *Monte Carlo and Molecular Dynamics Simulations in Polymer Science*, edited by K. Binder, Oxford University Press, New York, 1995
  - [13] R.G. Palmer, D. L. Stein, E. Abrahams, P.W. Anderson, Phys. Rev. Lett., **53**, 958 (1984)
  - [14] G. Iori, E. Marinari, G. Parisi, Europhys. Lett., **25**, 491 (1994)
  - [15] G.I. Nixon, G.W. Slater, Submitted to Europhys. Lett.; M. H. Cohen, G. Grest, Phys. Rev. B, **24**, 4091 (1981)
  - [16] A.T. Ogielski, Phys. Rev. B, **32**, 7384 (1985)
  - [17] J.P. Downey, Macromolecules, **27**, 2929 (1994)
  - [18] B.H. Zimm, R.W. Kilb, J. Polym. Sci., **37**, 19 (1959)